JACS
JOURNAL OF THE AMERICAN CHEMICAL SOCIETY
Communication
pubs.acs.org/JACS

Dynamic Optical Properties of $CH_3NH_3PbI_3$ Single Crystals As Revealed by One- and Two-Photon Excited Photoluminescence Measurements

Yasuhiro Yamada,[‡] Takumi Yamada,[‡] Le Quang Phuong, Naoki Maruyama, Hidetaka Nishimura, Atsushi Wakamiya, Yasujiro Murata, and Yoshihiko Kanemitsu*

Institute for Chemical Research, Kyoto University, Uji, Kyoto 611-0011, Japan

Supporting Information

ABSTRACT: The dynamic optical properties of perovskite $CH_3NH_3PbI_3$ single crystals were studied by means of time-resolved photoluminescence (PL) spectroscopy at room temperature. The PL peak under one-photon excitation exhibits a red-shift with elapsing time, while two-photon PL is time-independent and appears at lower energy levels. The low-energy two-photon PL can be attributed to emissions from the localized states because of strong band-to-band absorption and photon re-absorption of the emitted light in the interior region. We revealed that the PL behaviors can be explained by the diffusion of photocarriers generated in the near-surface region to the interior region. The excitation fluence dependence of the one-photon PL dynamics is also discussed in terms of the electron−hole radiative recombination and carrier diffusion effects.

Halide perovskite semiconductors of the form AMX_3 (A = CH_3NH_3, Cs, etc.; M = Pb, Sn; X = Cl, Br, I) have recently emerged as a promising class of materials for solar cell applications. In particular, since their first appearance in 2009 as light-absorbing materials for sensitized solar cells, $MAPbX_3$-based perovskites (MA = CH_3NH_3) have attracted attention because of their rapid increase in photoconversion efficiency.[1,2] The long carrier lifetime and, consequently, the long carrier diffusion length are regarded as being key features leading to the advanced photovoltaic properties of $MAPbX_3$-based solar cells.[3,4] Time-resolved spectroscopy revealed that the carrier lifetime under weak photoexcitation of an $MAPbI_3$ thin film is determined by the defect density.[5,6] Thus, the long carrier lifetime indicates the small defect density of perovskite semiconductors, which is supported by the theoretical finding that very few deep-level defects are formed in $MAPbI_3$ perovskite semiconductors.[7] Actually, a long diffusion length, exceeding 1 μm, has been reported in $MAPbX_3$, as determined by time-resolved photoluminescence (PL) spectroscopy,[3,8,9] while the long carrier lifetime (or long diffusion length) is in good correlation with the high photoconversion efficiency.[2]

To date, the optical properties of perovskite semiconductors have been studied using thin-film samples, which usually exhibit a grain structure (typically around 1 μm). However, it is considered that the grain structures have a major impact on the carrier diffusion and recombination in $MAPbX_3$ thin films. In addition, since trap states are more easily formed at the grain boundaries, relative to inside grains, the optical and electronic properties of thin-film samples could be dominated by extrinsic defects. In fact, observations have shown that the optical spectrum and dynamics are changed by the defect states in perovskite thin films.[10] Thus, to clarify the intrinsic properties of perovskite semiconductors, it is necessary to perform optical measurements on bulk crystals, which are free from grain boundaries and would be expected to have a lower defect density than a thin film. Although large-size $MAPbI_3$ single crystals have been recently fabricated,[11] their optical properties and photocarrier recombination processes remain unclear.

In this Communication, we describe the fabrication of $MAPbI_3$ single crystals and the study of their optical properties by means of time-resolved PL measurements under one- and two-photon excitation. The one-photon PL (1-PL) peak exhibits a red-shift with the passing of time in a single crystal, in contrast to the thin-film samples. This observation suggests that the spatial distribution of carriers is an important factor in the PL mechanism of a single crystal. By comparing the one- and two-photon photoluminescence excitation (PLE) spectra, we confirm that the bandgap energy is the same for both the near-surface and interior regions, and reveal that the carrier diffusion and photon re-absorption effects dominate the PL behaviors in $MAPbI_3$ single crystals. Our findings enable a deeper understanding of the physics of the photoconversion processes occurring in perovskite solar cells.

Single crystals of $MAPbI_3$ were obtained from a hot solution of γ-butyrolactone, by growing for 3 days (see Supporting Information (SI) for details). It is known that $MAPbI_3$ exhibits phase transitions at T_C = 327.4 K (cubic/tetragonal) and 162.2 K (tetragonal/orthorhombic).[12] Given that perovskite solar cells are used at room temperature (tetragonal phase), an X-ray crystal structural analysis was performed on the grown single crystal at 252 K (−20 °C). Although Baikie et al. reported that the crystal structure of $MAPbI_3$ at room temperature exhibits a less symmetrical space group of $I4/m$,[13] we were able to solve the structure with a space group of $I4/mcm$, in accordance with the results presented in a recent report.[14] Figure 1a shows an ORTEP drawing of the single-crystal X-ray structure of $MAPbI_3$ at −20 °C. Our X-ray diffraction analysis confirmed that the

Received: April 30, 2015
Published: August 11, 2015

DOI: 10.1021/jacs.5b04503
J. Am. Chem. Soc. 2015, 137, 10456−10459

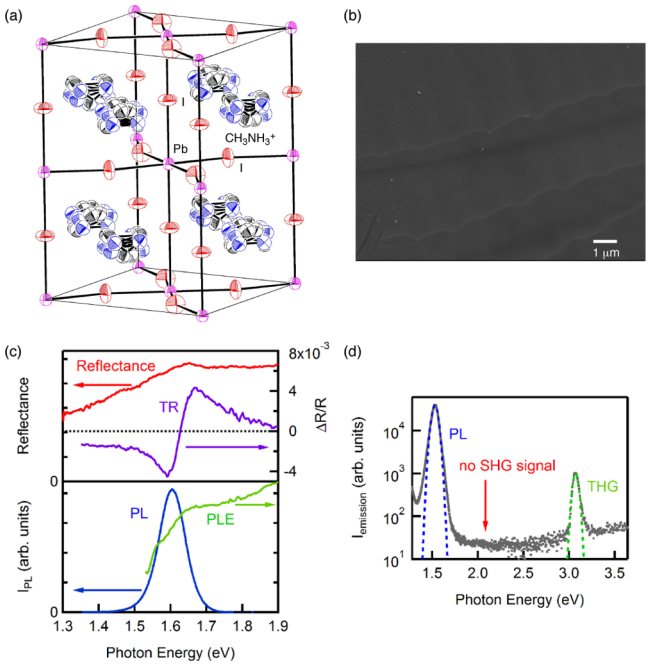

Figure 1. (a) ORTEP drawing of single-crystal X-ray structure of $MAPbI_3$ at −20 °C (thermal ellipsoids at 50% probability). (b) SEM image of cleaved surface of $MAPbI_3$ single crystal. (c) Reflectance, TR, PL, and PLE spectra. Excitation energy for PL and TR, 1.80 eV; PLE monitored at 1.50 eV. (d) Emission spectra under excitation at 1.03 eV.

samples used in the optical measurements described below were single crystals.

For scanning electron microscopy (SEM) and optical measurements, we cleaved the single crystal to obtain a fresh surface. Figure 1b shows a typical SEM image of the cleaved surface of a single crystal. The surface appears very smooth and clean. Note that the crystal morphology exhibits only a slight spatial dependence, while the optical properties are independent of the monitored position.

We studied the near-band-edge optical properties of $MAPbI_3$ single crystals at room temperature. Figure 1c shows the reflectance, transient reflectance (TR), PL, and PLE spectra. The reflectance spectrum shows a broad peak at around 1.63 eV, indicating the bandgap energy. To accurately determine the band gap energy, we measured the TR spectrum immediately after excitation (11 ps), with a pump excitation of 1.80 eV. The TR spectrum exhibits a typical photobleaching signal shape and is almost independent of the delay between 0 and 2 ns. The zero-crossing energy of 1.63 eV corresponds to the bandgap energy. The estimated bandgap energy of the $MAPbI_3$ single crystal is slightly larger than that which we reported previously for thin films (1.61 eV).[15] The PL spectrum peaks at 1.60 eV, which is almost the same as for a thin film.[16] This PL has been assigned as the band-to-band recombination of photoexcited electrons and holes.[13,16] The PLE spectrum monitored at 1.50 eV has two onsets at about 1.55 and 1.6 eV. The higher-energy onset is consistent with the bandgap energy. The double-onset structure of the PLE spectrum points to the complex near-band-edge optical properties of the $MAPbI_3$ single crystals.

Moreover, we conducted second harmonic generation (SHG) spectroscopy to evaluate the inversion symmetry of our $MAPbI_3$ single crystal, because it has been proposed that the ferroelectricity of $MAPbI_3$ plays an important role in current−voltage hysteresis of perovskite solar cells.[17] It is well known that a SHG signal appears when the inversion symmetry is broken, as occurs in ferroelectric materials,[18] as well as at surfaces and interfaces.[19] As shown in Figure 1d, no SHG signal was observed, even after a poling electric field (∼1 kV/cm) was applied, while strong third harmonic generation and PL signals due to two-photon absorption were observed. The lack of a SHG signal implies that our $MAPbI_3$ single crystals neither are ferroelectric nor contain grains that interfere with the inversion symmetry. This observation clearly eliminates the possibility of macroscopic ferroelectricity in $MAPbI_3$. However, it remains a possibility that ferroelectric domains are of a size below the laser wavelength.

We conducted the time-resolved PL measurements in $MAPbI_3$ single crystals using a streak camera. Figure 2a shows the PL

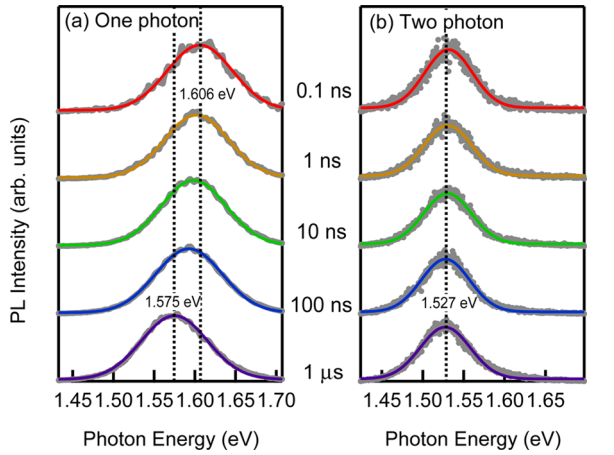

Figure 2. Time-resolved PL spectra under excitation of (a) 1.80 eV (one-photon excitation) and (b) 1.20 eV (two-photon excitation).

spectra for different delays with excitation at 1.80 eV, which is sufficiently above the bandgap energy of 1.63 eV. The PL spectrum peaks at around 1.606 eV immediately after excitation. As the delay increases, the PL peak red-shifts. This behavior is in contrast to that of the thin film samples, whereby the shape of the PL spectrum is temporary unchanged.[5] This difference between single crystals and thin films suggests that the spatial distribution of photocarriers plays an important role in the PL properties. The photoexcited carriers, which initially are generated in the near-surface region (∼penetration depth), diffuse to the interior state with the elapse of time, thus giving rise to the PL red-shift. The radiative recombination and light emission processes in the near-surface and interior regions should be different.

To clarify the spatial effect on the PL peak shift, we compared the time-resolved PL spectra produced by one-photon and two-photon excitation. The initial PL under one-photon excitation reflects the near-surface region up to the penetration depth (around 250 nm),[5] and the PL from the interior region will appear as the carriers diffuse to the interior region. On the other hand, under two-photon excitation, the photocarriers are generated within the laser spot (around 100 μm). Because of the widespread carrier distribution relative to the typical diffusion length of $MAPbI_3$, the two-photon PL (2-PL) is regarded as reflecting the interior region, while the carrier diffusion processes are negligible. As shown in Figure 2b, almost no PL peak shift is observed under two-photon excitation, in contrast to the 1-PL. Moreover, the 2-PL peak energy was 1.53 eV, which is much smaller than that obtained with 1-PL (around 1.60 eV). Note that we confirmed the two-photon absorption under 1.20 eV excitation by checking the dependence of the PL intensity on

DOI: 10.1021/jacs.5b04503
J. Am. Chem. Soc. 2015, 137, 10456−10459

the excitation power (data not shown). We also measured the three-photon PL (excited at 0.6 eV, see Figure S1 in SI), which exhibits the same spectrum shape as 2-PL. This observation ensures that the difference between 1-PL and 2-PL does not originate from different selection rules for one- and two-photon optical absorption.

We summarize the temporal change of PL peak energies under one- and two-photon excitation in Figure 3a. The 1-PL peak

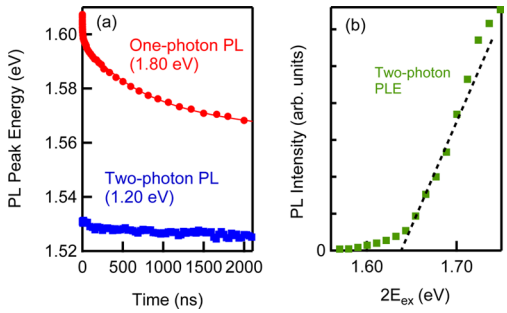

Figure 3. (a) One-photon and two-photon PL peak energies as a function of elapsed time. (b) Two-photon PLE spectrum. The broken line is for reference only.

gradually approaches the 2-PL peak. Two possibilities are considered in the interpretation of the different PL behaviors of the near-surface and interior regions. One is that the bandgap energies of the near-surface and interior regions are different. To check this possibility, we measured the two-photon PLE spectra, shown in Figure 3b. The onset energy of two-photon PLE is located at 1.64 eV, which is in good agreement with the bandgap energy determined by the optical spectra under one-photon excitation (see Figure 1c). This clearly indicates that the bandgap energy is independent of the depth relative to the surface in $MAPbI_3$ single crystals.

Rather, we regard the photon re-absorption effect as dominating the carrier recombination and light-emission processes in the interior region. The high-energy part of the band-to-band PL emitted in the interior region is immediately re-absorbed and cannot readily escape from the crystal because of the large band-to-band absorption and small Stokes shift. Thus, the lower energy part of the PL is emphasized in the single crystals, which results in the PL red-shift in comparison with the original PL spectrum. On the other hand, any band-to-band emission in the near-surface region can easily escape from the crystal. Given this scenario, photocarriers in the near-surface region emit high-energy PL, and the 1-PL peak red-shifts with the photocarrier diffusion to the interior region. We confirmed by a simple numerical simulation that 1-PL red-shift is well accounted for by considering photon re-absorption and one-dimensional photocarrier diffusion. Here we used the carrier mobility of 50 $cm^2/(V{\cdot}s)$.[20] We plotted the calculated PL spectrum and spatial distribution of photocarriers at 0, 1, 10, and 100 ns and 1 μs in Figure 4 (see SI for details). The calculated results well reproduce the experimental results. Note that a few percent of the photocarriers still remain in the near-surface region even at 1 μs. Thus, the band-edge emission from the near-surface region is predominantly observed.

Two-photon excitation produces photocarriers only in the interior region. Thus, the band-edge emission is almost entirely re-absorbed. This means that the lower PL peak energy under two-photon excitation cannot be accounted for by the re-absorption effect. We believe that the defect PL is dominant in 2-

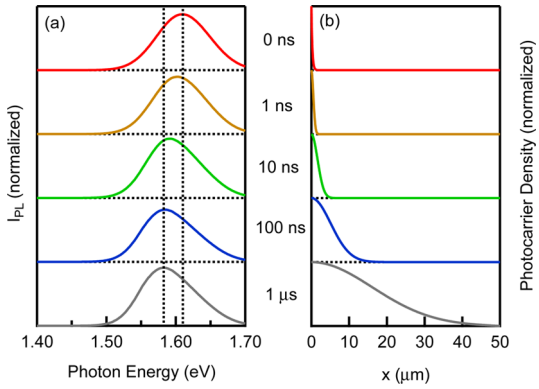

Figure 4. (a) Calculated PL spectrum and (b) photocarrier density profile at 0, 1, 10, and 100 ns and 1 μs.

PL. This is why the 1-PL spectrum shape is different from that of 2-PL.

It should be emphasized that the importance of the re-absorption effect has been recognized in high-quality semiconductors such as GaAs, for application to solar cells and light-emitting diodes.[21] Therefore, we can conclude that the PL behaviors can be fully explained by the carrier diffusion and re-absorption effects in $CH_3NH_3PbI_3$ single crystals.

1-PL decay dynamics are also determined by the carrier diffusion effect. Figure 5a shows the decay dynamics of 1-PL and

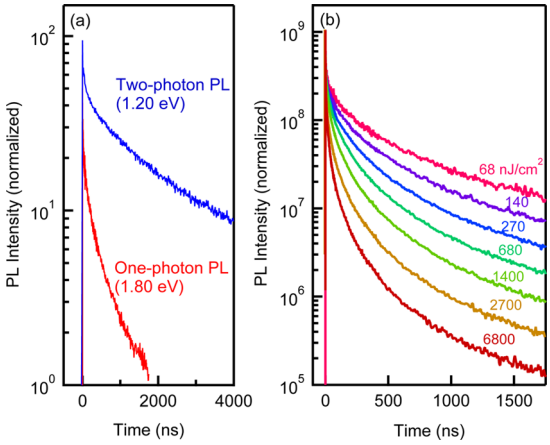

Figure 5. (a) PL decay dynamics under one-photon and two-photon excitation. (b) 1-PL dynamics for different excitation fluences, monitored at 1.62 eV.

2-PL. Excitation fluencies were 68 nJ/cm^2 and 50 $\mu J/cm^2$, respectively. We confirmed that the PL dynamics are almost independent of excitation fluencies below these excitation levels. 1-PL was monitored at the higher energy (1.62 eV), which is considered to reflect the recombination of the near-surface photocarriers. The excitation fluence for one-photon excitation was 68 nJ/cm^2. The 1-PL intensity exhibits rapid decay within 20 ns and a slow-decay component with a decay time of 500 ns. We believe that the fast decay of the 1-PL results from the carrier diffusion because this fast decay is not observed in thin films.[5] Because PL intensity is in proportion to the carrier density in $MAPbI_3$,[5] a decrease in carrier density by diffusion causes the reduction in PL intensity. It should be commented that the fast PL decay is more or less contributed by surface defects. On the other hand, the 2-PL exhibits a long-lived exponential decay, with a lifetime of 4 μs, in addition to the weak fast decay component.

DOI: 10.1021/jacs.5b04503
J. Am. Chem. Soc. 2015, 137, 10456−10459

Note that the 2-PL lifetime does not correspond to the intrinsic carrier recombination lifetime in the interior region because the light emission and re-absorption processes dominate the PL lifetime.

To gain a fuller understanding of the photocarrier recombination dynamics in $MAPbI_3$ single crystals, we studied the excitation fluence dependence of the PL decay dynamics. For thin films, the PL dynamics are well explained by a simple rate equation which considers electron−hole radiative recombination and single-carrier trapping.[5] Auger recombination and other higher-order processes are negligible in this range of excitation fluence.[22] Figure 5b shows the 1-PL dynamics for different values of excitation fluence. As the excitation fluence increases, the PL decays more quickly. The PL dynamics, which are dependent on the excitation fluence, are regarded as originating from electron−hole bimolecular recombination. Therefore, we can conclude that the photocarrier dynamics in $MAPbI_3$ single crystals are dominated by carrier diffusion, electron−hole radiative recombination, and single-carrier trapping.

In conclusion, we studied the dynamic behavior of photocarriers in $MAPbI_3$ single crystals. While the 1-PL exhibits a red-shift with elapsing time, 2-PL does not exhibit any immediate change. We found that the bandgap energies are the same in the near-surface and interior regions, but the PL mechanisms are different. We demonstrated by a numerical simulation that the spectral change originates from the effects of carrier diffusion and photon re-absorption. The fast 1-PL decay dynamics are also dominated by the carrier diffusion process. The large impact of the carrier diffusion effects suggests a high carrier mobility for $MAPbI_3$, which reaches more than 50 $cm^2/(V{\cdot}s)$. Our results highlight the importance of the carrier diffusion effect to the interpretation of the optical properties of $MAPbI_3$ single crystals and thick films. Our findings provide essential insights into the dynamic carrier behaviors of $MAPbI_3$ for solar-cell applications.

■ ASSOCIATED CONTENT

Supporting Information

The Supporting Information is available free of charge on the ACS Publications website at DOI: 10.1021/jacs.5b04503.

Sample preparation and experimental method (PDF)
X-ray crystallographic data for $MAPbI_3$(CIF)

■ AUTHOR INFORMATION

Corresponding Author

*kanemitu@scl.kyoto-u.ac.jp

Author Contributions

‡Y.Y and T.Y. contributed equally.

Notes

The authors declare no competing financial interest.

■ ACKNOWLEDGMENTS

Part of this work was supported by the Sumitomo Electric Industries Group CSR Foundation (to Y.Y. and Y.K.), JST-PRESTO (to A.W.), and JST-CREST (to Y.K.). We thank Prof. T. Sasamori and Prof. N. Tokitoh (Kyoto University) for X-ray crystal structure analysis of $MAPbI_3$ and Prof. K. Matsuda (Kyoto University) for SEM measurement, respectively.

■ REFERENCES

(1) (a) Kojima, A.; Teshima, K.; Shirai, Y.; Miyasaka, T. *J. Am. Chem. Soc.* **2009**, *131*, 6050. (b) Im, J.-H.; Lee, C.-R.; Lee, J.-W.; Park, S.-W.; Park, N.-G. *Nanoscale* **2011**, *3*, 4088. (c) Kim, H.-S.; Lee, C.-R.; Im, J.-H.; Lee, K.-B.; Moehl, T.; Marchioro, A.; Moon, S.-J.; Humphry-Baker, R.; Yum, J.-H.; Moser, J. E.; Grätzel, M.; Park, N.-G. *Sci. Rep.* **2012**, *2*, 591. (d) Lee, M. M.; Teuscher, J.; Miyasaka, T.; Murakami, T. N.; Snaith, H. J. *Science* **2012**, *338*, 643. (e) Burschka, J.; Pellet, N.; Moon, S.-J.; Humphry-Baker, R.; Gao, P.; Nazeeruddin, M. K.; Grätzel, M. *Nature* **2013**, *499*, 316. (f) Docampo, P.; Ball, J. M.; Darwich, M.; Eperon, G. E.; Snaith, H. J. *Nat. Commun.* **2013**, *4*, 2761. (g) Green, M. A.; Emery, K.; Hishikawa, Y.; Warta, W.; Dunlop, E. D. *Prog. Photovoltaics* **2015**, *23*, 1.

(2) Zhou, H.; Chen, Q.; Li, G.; Luo, S.; Song, T.; Duan, H.; Hong, Z.; You, J.; Liu, Y.; Yang, Y. *Science* **2014**, *345*, 542.

(3) Stranks, S. D.; Eperon, G. E.; Grancini, G.; Menelaou, C.; Alcocer, M. J. P.; Leijtens, T.; Herz, L. M.; Petrozza, A.; Snaith, H. J. *Science* **2013**, *342*, 341.

(4) (a) Xing, G.; Mathews, N.; Sun, S.; Lim, S. S.; Lam, Y. M.; Grätzel, M.; Mhaisalkar, S.; Sum, T. C. *Science* **2013**, *342*, 344. (b) Marchioro, A.; Teuscher, J.; Friedrich, D.; Kunst, M.; van de Krol, R.; Moehl, T.; Grätzel, M.; Moser, J.-E. *Nat. Photonics* **2014**, *8*, 250. (c) Zhao, Y.; Nardes, A. M.; Zhu, K. *J. Phys. Chem. Lett.* **2014**, *5*, 490.

(5) Yamada, Y.; Nakamura, T.; Endo, M.; Wakamiya, A.; Kanemitsu, Y. *J. Am. Chem. Soc.* **2014**, *136*, 11610.

(6) (a) Wehrenfennig, C.; Liu, M.; Snaith, H. J.; Johnston, M. B.; Herz, L. M. *Energy Environ. Sci.* **2014**, *7*, 2269. (b) D'Innocenzo, V.; Kandada, A. R. S.; De Bastiani, M.; Gandini, M.; Petrozza, A. *J. Am. Chem. Soc.* **2014**, *136*, 17730.

(7) Yin, W.-J.; Shi, T.; Yan, Y. *Appl. Phys. Lett.* **2014**, *104*, 063903.

(8) Xiao, Z.; Dong, Q.; Bi, C.; Shao, Y.; Yuan, Y.; Huang, J. *Adv. Mater.* **2014**, *26*, 6503.

(9) Dong, Q.; Fang, Y.; Shao, Y.; Mulligan, P.; Qiu, J.; Cao, L.; Huang, J. *Science* **2015**, *347*, 967.

(10) (a) Wu, X.; Trinh, M. T.; Niesner, D.; Zhu, H.; Norman, Z.; Owen, J. S.; Yaffe, O.; Kudisch, B. J.; Zhu, X.-Y. *J. Am. Chem. Soc.* **2015**, *137*, 2089. (b) Yamada, Y.; Endo, M.; Wakamiya, A.; Kanemitsu, Y. *J. Phys. Chem. Lett.* **2015**, *6*, 482.

(11) (a) Dang, Y.; Liu, Y.; Sun, Y.; Yuan, D.; Liu, X.; Lu, W.; Liu, G.; Xia, H.; Tao, X. *CrystEngComm* **2015**, *17*, 665. (b) Shi, D.; Adinolfi, V.; Comin, R.; Yuan, M.; Alarousu, E.; Buin, A.; Chen, Y.; Hoogland, S.; Rothenberger, A.; Katsiev, K.; Losovyj, Y.; Zhang, X.; Dowben, P. A.; Mohammed, O. F.; Sargent, E. H.; Bakr, O. M. *Science* **2015**, *347*, 519. (c) Dong, Q.; Fang, Y.; Shao, Y.; Mulligan, P.; Qiu, J.; Cao, L.; Huang, J. *Science* **2015**, *347*, 967. (d) Fang, H.-H.; Raissa, R.; Abdu-Aguye, M.; Adjokatse, S.; Blake, G. R.; Even, J.; Loi, M. A. *Adv. Funct. Mater.* **2015**, *25*, 2378.

(12) Poglitsch, A.; Weber, D. *J. Chem. Phys.* **1987**, *87*, 6373.

(13) Baikie, T.; Fang, Y.; Kadro, J. M.; Schreyer, M.; Wei, F.; Mhaisalkar, S. G.; Grätzel, M.; White, T. J. *J. Mater. Chem. A* **2013**, *1*, 5628.

(14) Dang, Y.; Liu, Y.; Sun, Y.; Yuan, D.; Liu, X.; Lu, W.; Liu, G.; Xia, H.; Tao, X. *CrystEngComm* **2015**, *17*, 665.

(15) Yamada, Y.; Nakamura, T.; Endo, M.; Wakamiya, A.; Kanemitsu, Y. *Appl. Phys. Express* **2014**, *7*, 032302.

(16) Yamada, Y.; Nakamura, T.; Endo, M.; Wakamiya, A.; Kanemitsu, Y. *IEEE J. Photovolt.* **2015**, *5*, 401.

(17) (a) Kutes, Y.; Ye, L.; Zhou, Y.; Pang, S.; Huey, B. D.; Padture, N. P. *J. Phys. Chem. Lett.* **2014**, *5*, 3335. (b) Fan, Z.; Xiao, J.; Sun, K.; Chen, L.; Hu, Y.; Ouyang, J.; Ong, K. P.; Zeng, K.; Wang, J. *J. Phys. Chem. Lett.* **2015**, *6*, 1155.

(18) Ok, K. M.; Chi, E. O.; Halasyamani, P. S. *Chem. Soc. Rev.* **2006**, *35*, 710.

(19) Cao, H.; Wu, J. Y.; Ong, H. C.; Dai, J. Y.; Chang, R. P. H. *Appl. Phys. Lett.* **1998**, *73*, 572.

(20) Stoumpos, C. C.; Malliakas, C. D.; Kanatzidis, M. G. *Inorg. Chem.* **2013**, *52*, 9019.

(21) (a) Schnitzer, I.; Yablonovitch, E.; Caneau, C.; Gmitter, T. J. *Appl. Phys. Lett.* **1993**, *62*, 131. (b) Miller, O. D.; Yablonovitch, E.; Kurtz, S. R. *IEEE J. Photovolt.* **2012**, *2*, 303.

(22) Wehrenfennig, C.; Eperon, G. E.; Johnston, M. B.; Snaith, H. J.; Herz, L. M. *Adv. Mater.* **2014**, *26*, 1584.

DOI: 10.1021/jacs.5b04503
J. Am. Chem. Soc. 2015, 137, 10456−10459